



Real-Time Analysis for Enhancement of Photovoltaic Panel Efficiency and Quality

Bachir Zine^{1*}, Chouaib Labiod¹, Kamel Srairi², Amel Benmouna^{3,4,5}, Mohamed Becherif^{3;4,5}, Abderrahmane Khechekhouche¹, Blaise Ravelo⁶, Mohamed Naoui⁷

¹University of Eloued, Algeria

²University of Biskra, Algeria

³University Bourgogne Franche-Comte, Belfort, France

⁴School of Business and Engineering, Belfort, France

⁵University Tenaga Nasional, Kajang, Selangor, Malaysia

⁶Nanjing University of Information Science and Technology (NUIST), Nanjing, Jiangsu, China

⁷University of Gabés, Gabés, Tunisia

*Correspondence: E-mail: zine-bachir@univ-eloued.dz

ABSTRACT

This study addressed the quality assessment of photovoltaic (PV) panels by analyzing their efficiency and electrical power under varying environmental conditions. A sophisticated algorithm was developed to extract and analyze PV panel voltage and current data in a complex manner, allowing the identification of key parameters such as open circuit voltage (Voc), short circuit current (Isc), and peak electrical power. These parameters were compared to the input power to accurately determine the panel efficiency. The novelty of this approach lies in its real-time implementation using a DC/DC (buck-boost) converter equipped with precise voltage and current sensors and running on a TMS320f379D board, linking theoretical knowledge with practical results. Experimental results demonstrated that temperature and irradiation significantly influence PV performance. With a 10°C increase in temperature, it resulted in a 5-10% decrease in output power, while a 100 W/m² increase in irradiation resulted in a 10-15% increase in output power. The study highlights the importance of considering both temperature and irradiation variations to optimize PV system design and operation, providing a robust method to assess PV panel quality in real-time.

ARTICLE INFO

Article History:

Submitted/Received 01 Jun 2024

First Revised 06 Aug 2024

Accepted 25 Sep 2024

First Available online 26 Sep 2024

Publication Date 01 Dec 2024

Keyword:

Efficiency evaluation,
Electrical power output,
Photovoltaic panels,
Radiation impact,
Real-time analysis,
Temperature effects.

1. INTRODUCTION

Renewable energy, particularly solar power, is crucial for tackling environmental issues. Photovoltaic (PV) systems efficiently convert sunlight into clean electricity but require adherence to quality standards and optimal operational conditions for maximum performance. Ensuring high standards in manufacturing and using advanced techniques, like transistor driving for electronic inverters, is essential for reliable and efficient PV system operation. Recent studies have focused on enhancing the performance and reliability of PV systems by integrating innovative approaches to address key challenges. They investigated the impact of dust accumulation, temperature variations, and radiation levels on PV panel efficiency, showing that dust can reduce energy production by about 34.65% and temperature increases can decrease energy production by 5 to 10% for every 10 °C rise. To tackle these issues, a real-time data acquisition system and advanced algorithms were developed to monitor and analyze PV panel performance, including open-circuit voltage, short-circuit current, and maximum power point (MPP). Additionally, new methods such as principal component analysis (PCA) for shading fault diagnosis and the Sailfish Optimizer (SFO) for improved PV modeling have contributed to more robust fault assessment and monitoring, ensuring better energy production under various conditions (Largot et al., 2024; Atiyah et al., 2023; Ghodbane et al., 2023; Medekhel et al., 2022).

Fault detection remains critical to maintaining PV system efficiency and preventing potential hazards. For example, Dhimish et al. (2018) demonstrated effective algorithms for detecting various types of faults, including single and double faulty modules and partial shading, while Eskandari et al. (2021) validated techniques for accurately differentiating between line-to-line (LL) and line-to-ground (LG) faults, achieving high accuracy rates. These advancements in fault detection and diagnosis are pivotal for enhancing the overall reliability and efficiency of PV systems.

Research by Ji et al. (2017) emphasized the importance of automatic fault detection to prevent efficiency loss and reduce the risk of fires. The study proposed methods for classifying various faults, including open circuits, mismatches, and short circuits, based on the analysis of current-voltage (I-V) curves. Zhao et al. (2013) highlighted the dangers of line-to-line faults, which pose safety risks and can reduce system reliability and efficiency. Zhang et al. (2021) proposed a robust fault diagnosis method, tested through four case studies that demonstrated significant discrimination ability, adaptability, and practicality for real-world applications. Zhu et al. (2019) showed a study of the joint temporal-spatial distribution of array output in large-scale PV plants examining how energy production varies over time and across the array layout. By analyzing these variations, the study helps in identifying faults such as shading, equipment degradation, and mismatched strings, enhancing fault diagnosis and maintenance efficiency, and ultimately improving the overall performance and reliability of PV systems.

Further research by Kim et al. (2021) explored quantitative output analysis for fault detection in PV systems. Paul et al. (2016) developed a strategy for fault classification and isolation to ensure continuous operation without shutting down the entire system. Momeni et al. (2020) successfully identified and fixed various faults under diverse environmental conditions typical for PV arrays. Yang et al. (2013) investigated the control options available for single-phase PV systems when dealing with grid faults.

Studies by Bharadwaj et al. (2016) focused on sequential optimization for accurate power output estimation in aging solar PV systems, while Vinod (2008) assessed the electrical quality of metal contacts on solar cells by measuring total ohmic losses. Movla et al. (2015) identified

that variations in electrical characteristics, particularly thickness, can significantly affect solar cell performance.

The performance and reliability of PV systems are critically influenced by various environmental factors and system design parameters. Accurate identification and optimization of these parameters are essential to maximize solar energy conversion efficiency. [Zagrouba et al. \(2010\)](#) used genetic algorithms to efficiently identify parameters of solar PV cells and modules, demonstrating a significant impact on maximizing energy extraction under varying conditions. Similarly, understanding the diurnal and environmental characteristics of solar panels is crucial for improving PV performance, as highlighted by [Kattakayam et al. \(1996\)](#), who used a PC-AT plug-in card to analyze these effects. Innovations in PV system integration, such as installing PV panels on greenhouse roofs, offer a dual benefit of energy production and improved agricultural productivity, as explored by [Trypanagnostopoulos et al. \(2017\)](#). Furthermore, the work of [Zaimi et al. \(2019\)](#) highlights the need to consider the combined effects of solar radiation and panel junction temperature on all model parameters, which is essential to accurately predict peak power and PV efficiency under non-standard conditions. The dynamic thermal behavior of PV panels, a key aspect of their performance, has also been studied by [Roger and Maguin \(1982\)](#), who developed simulation models that integrate these thermal effects to better predict panel production under various environmental scenarios.

In addition to optimizing design and operating parameters, continuous monitoring and diagnostics play a critical role in maintaining PV system performance. [Tina et al. \(2015\)](#) highlighted the importance of robust monitoring systems to diagnose and resolve operational issues in PV power plants, thereby improving system reliability and lifetime. As PV installations grow, the complexity of fault detection and classification also increases, requiring advanced methods to maintain system efficiency. [Hong and Pula \(2022\)](#) provided a comprehensive review of contemporary fault detection techniques, which are crucial for the proactive maintenance of large-scale PV installations.

The main objective of this study was to investigate the effects of temperature and solar radiation on the performance of PV panels, providing a comprehensive analysis supported by quantitative data. This research aimed to deepen the understanding of how these environmental factors influence PV efficiency and production, highlighting key performance indicators and identifying areas for optimization. By examining these effects, the study provides valuable information to improve the design and operation of PV systems, thereby improving energy yield under various conditions.

2. METHODS

2.1. Experimental setup

Figure 1 represents our experiment to study the performance of PV panels. The main components include the PV panel itself, a temperature sensor, an oscilloscope, a multimeter, a power supply, a microcontroller, a proprietary board, current and voltage sensors, and a PC. Potential research objectives include measuring efficiency and output power, analyzing I-V characteristics, studying dynamic response, studying system integration, and assessing reliability and degradation. By analyzing the collected data, researchers can gain valuable insights into the behavior of PV panels and contribute to the advancement of renewable energy technologies.

Table 1 summarizes the main experimental parameters giving more details about configuration and settings used during the validation process. These parameters are

important in providing a background against which the proposed strategy can be tested and validated under different PV systems states.

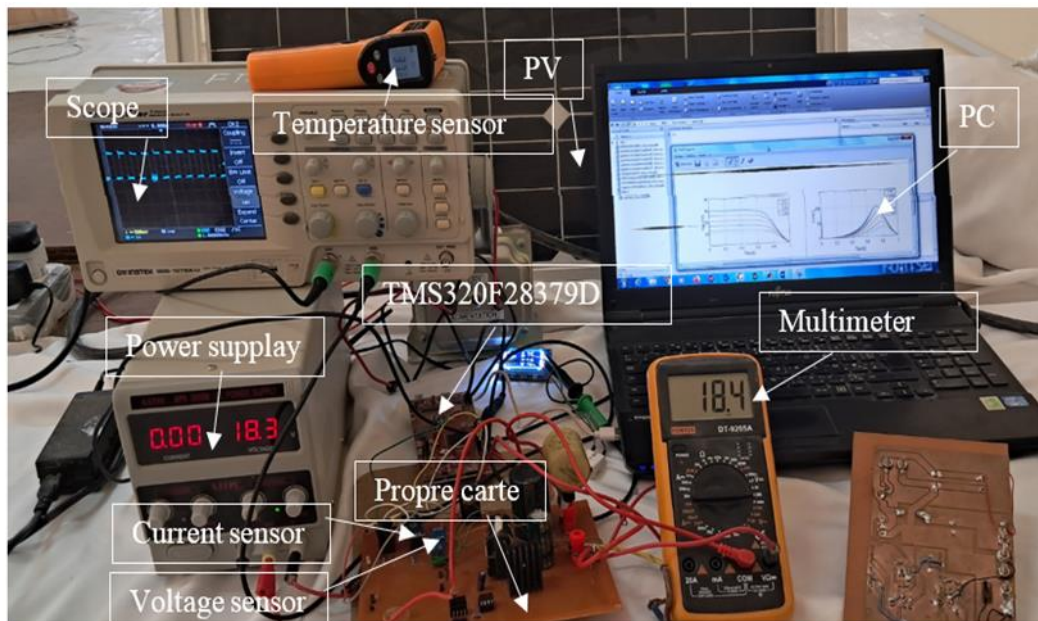


Figure 1. Test bench.

Table 1. Experimental parameters

Parameter	Numerical Value
DC-link Voltage [V]	24
Sampling frequency [kHz]	10
Reference frequency [Hz]	50
Resistance load [Ω]	3.4
Inductance load [mH]	20
DC-link bus capacitor (C1, C2) [μF]	3300

2.2. Proposed model

This method involves measuring current, voltage, and solar radiation intensity to *get all* points related to solar panel characteristics which need changes in electric load covering them, and this is achieved using an electronic power transformer that converts DC into AC, and also by varying activation angle α through microcontroller, this is done by algorithm which depends on sequential changing of angle α to clear all these points as shown in **Figure 2**.

Each transistor gate activation angle of the electronic transformer is obtained. Then calculate the voltage for the open circuit and current for the short circuit and yield from all its sensors' data (current, voltage, intensity of solar radiation). In this method, a DC-DC converter is used for extracting information from the solar panel. The duty cycle represents the ratio between the ON time of the converter and the complete period. When the duty cycle is varied from 0 to 1, the output voltage or current can be adjusted by the converter accordingly.

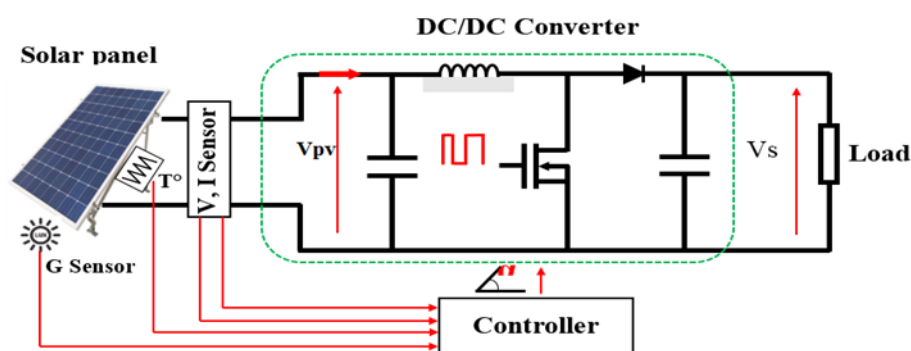


Figure 2. Principle diagram of the device.

2.3. Statistical and signal processing techniques

Figure 3 classifies PV FDD methods into electrical and visual/thermal categories. Electrical methods analyze structured data such as I-V curves, while visual/thermal methods analyze unstructured images. The specific techniques for each category vary depending on the fault type and module configuration. Additional methods such as TDR, earth capacitance measurement, and spectrum analysis can also be used for fault detection and localization.

To determine and locate defective PV module arrays, the TDR (Time Domain Reflectometry), Earth Capacitance Measurement, and Spectrum Analysis methods can be used [23]. Different installation conditions may affect its efficiency; for example, types of materials employed in PV parts as well as their wiring.

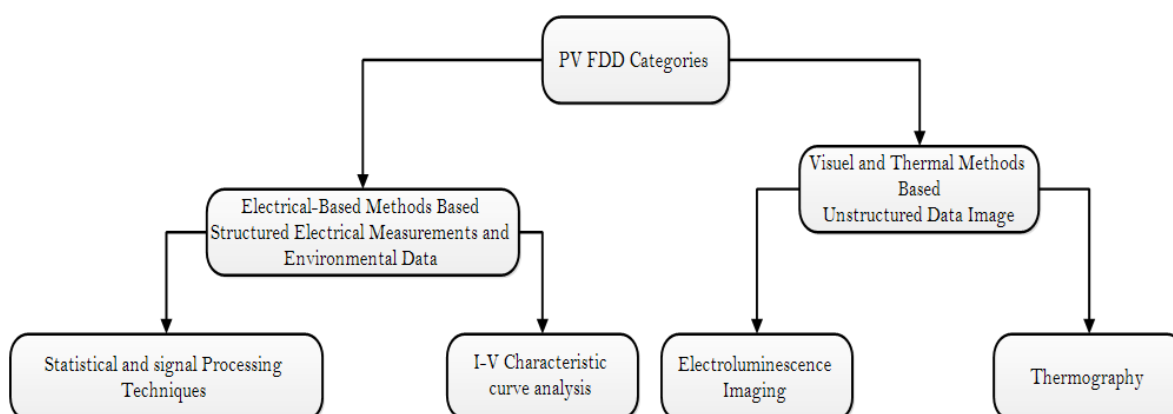


Figure 3. Categories of PV FDD and exemplars Hong and Pula (2022).

2.4. PV model

The equivalent circuit model in Figure 4 represents a PV panel using a current source, a diode, a series resistor, and a shunt resistor to model its electrical behavior. This simplified model is commonly used for analysis, simulation, and design purposes, providing a convenient representation of the complex relationship between current and voltage in PV panels Manno et al. (2021).

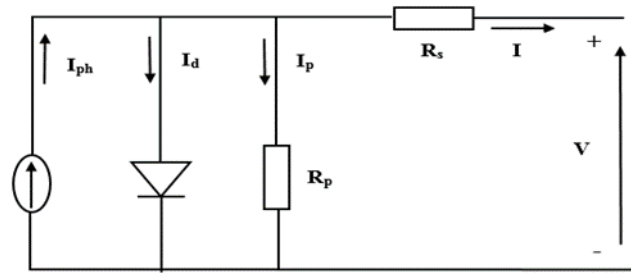


Figure 4. Equivalent circuit of real model for PV panel.

The current source (I_{ph}) is in parallel with the diode of an ideal solar cell which can be modeled as a solar PV device. All equations from (1) to (10) used in this work are given from the literature. Detailed information regarding the symbols is explained in **Table 2**.

Table 2. Nomenclatures.

Symbols/Abbreviations	Definition
I	Total current
I_{ph}	photocurrent
I_d	Dark current
I_s	Saturation current
Exp	Exponential function
q	Charge of an electron (approximately 1.6×10^{-19} coulombs).
V_{oc}	Open-circuit voltage
N_s	Emission coefficient of the diode
K	Boltzmann's constant (approximately 1.38×10^{-23} joules per kelvin)
T_0	Temperature of the diode
i_L	Current through the inductor
D	Duty cycle
di_L/dt	Rate of change of current with respect to time
A	Diode area
R_s	Series resistance
N_p	Number of cells connected in parallel
I_{sc}	Short circuit current
T_r	Reference temperature
G	solar irradiance
G_{ref}	Reference solar irradiance
I_{rs}	Reverse saturation current
E_g	This is the energy band gap of the semiconductor material used in the diode.
i_s	Source current
C_2	Capacitance
dV_s/dt	Represents the rate of change of the source voltage with respect to time
V_s	DC voltage used to power the component or circuit
L	Inductance

Equation (1) defines the output current of an ideal solar cell.

$$I = I_{ph} - I_d \quad (1)$$

Shockley's diode current equation is the main mathematical equation used to describe I-V (current-voltage) characteristics in a PV solar cell. This equation comes from semiconductor physics and can be written as Equation (2).

$$I_d = I_s \left[\exp\left(\frac{qV_{oc}}{N_s K A T_o}\right) - 1 \right] \quad (2)$$

To get the output current I of an ideal solar cell, I_d (diode current) should be substituted into equations (1) and (3).

$$I = I_{ph} - I_s \left[\exp\left(\frac{qV_{oc}}{N_s K A T_o}\right) - 1 \right] \quad (3)$$

When there are many PV modules in a solar PV system, R_p or parallel resistance starts being noticeable. Therefore, R_s or series resistance is considered because R_p is assumed infinite. Then, Equation (2) is modified for the diode current either to Equations (3) or (4) depending on context.

$$I_d = I_s \left[\exp\left(\frac{q(V+IR_s)}{N_s K A T_o}\right) - 1 \right] \quad (4)$$

$$I = I_{ph} - I_s \left[\exp\left(\frac{q(V+IR_s)}{N_s K A T_o}\right) - 1 \right] \quad (5)$$

Equation (5) can be changed if PV cells are connected in series-parallel configuration while calculating for the output current I . The modified equation is given by Equation (6).

$$I = N_p \times I_{ph} - N_p \times I_s \left[\exp\left(\frac{q(V+IR_s)}{N_s K A T_o}\right) - 1 \right] \quad (6)$$

$$I_{ph} = [I_{sc} + K_i(T_o - T_r)] \times \frac{G}{G_{ref}} \quad (7)$$

According to the above equations, many parameters have to be identified when simulating PV cells. The choice of the PV module requires different values for each model. One of the models proposed by [Vinod and Singh \(2018\)](#) is presented in Equations (8) and (9).

$$I_{rs} = \frac{I_{sc}}{\left[\exp\left(\frac{qV_{oc}}{N_s K A T_o}\right) - 1 \right]} \quad (8)$$

$$I_s = I_{rs} \frac{T_o}{T_r} 3 \exp\left[\left(\frac{qE_g}{AK}\right) \left(\frac{1}{T_r} - \frac{1}{T_o}\right)\right] \quad (9)$$

Temperature is an input parameter in solar PV systems, which is measured in degrees Celsius.

However, for precise mathematical representation of PV cells, temperature has to be expressed in Kelvin.

2.5. Buck-Boost Converter Model

The buck-boost converter circuit shown in **Figure 5** consists of an input voltage source, an inductor, capacitors, a diode, and a switch. It can operate in either continuous or discontinuous conduction mode. By controlling the duty cycle of the switch, the converter can produce an output voltage higher or lower than the input voltage, making it a versatile DC-DC converter topology.

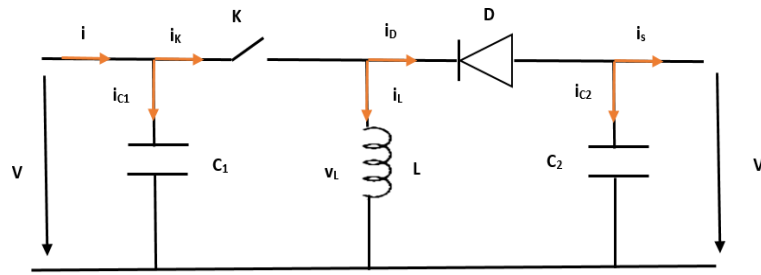


Figure 5. The electrical circuit of a Buck-Boost converter [Fadhel et al. \(2019\)](#).

The equation (10) in power electronics and transformer systems is called the "inductor current balance equation" or "inductor current equation." It is widely used for studying switching transformers such as buck transformers, boost transformers, and other types of switching power supplies.

$$i_L = \frac{1}{D} \left(i - c_1 \frac{dV}{dt} \right) \tag{10}$$

Equation (11) describes the relationship between switch current, inductor current, duty cycle, and rate of change of switch voltage during continuous conduction mode operation of a converter system. This formula helps to know about the behavior of switch current as well as gives insight into power dissipation, losses, and overall performance of the converter.

$$i_s = -(1 - D)i_L - c_2 \frac{dV_s}{dt} \tag{11}$$

Equation (12) represents the relationship between voltages across an inductor concerning a switch during continuous conduction mode operation of a converter system. It considers the value of inductance, rate of change inductor current, duty cycle, and voltage across the switch. Equation (12) is often used when analyzing or designing switching converters to understand how much voltage there will be across an inductor while it works. Many other related equations can be solved together with this one to optimize the design for converters, evaluate component voltage stresses, and find appropriate control parameters that would make the converter work efficiently.

$$V = \frac{1}{D} \left(L \frac{di_L}{dt} - (1 - D)V_s \right) \tag{12}$$

3. RESULTS AND DISCUSSION

3.1. MPPT algorithm for PV system

It is well known that when radiation decreases, it does to current. The same decrease can be seen in power output, which also declines accordingly. Voltage however only changes slightly; thus, indicating a lower sensitivity of voltage to radiation than current. Nevertheless, it should be understood that various electrical systems may respond differently to altered levels of radiation depending on their unique components and designs. To obtain data points that cover the entire range of characteristics possessed by different types of PV modules; it is necessary to change systematically duty cycle.

Figure 6 describes an MPPT algorithm for PV systems. It starts by initializing the parameters and measuring the PV voltage and current. It then iteratively calculates the power, compares it to the maximum power, and adjusts the duty cycle accordingly. The algorithm continues until the maximum power point is reached or the duty cycle limit is exceeded. Finally, it prints the results of the maximum power, open-circuit voltage, and short-circuit current.

The converter can sample different points of the solar panel by changing the duty cycle. This makes it possible to gather information under various conditions such as different solar radiation intensities and various electrical loads. Then, the data collected, which includes current, voltage, and solar radiation intensity is used for computation and interpretation purposes. By covering all possible duty cycles ranging from 0 to 1, this method will collect data at every point on the solar panel characteristic curve. This wide-ranging data acquisition will enable better comprehension of how well PVs perform and allow for more efficient adjustments aimed at maximizing their efficiencies. In general terms, a DC-DC converter with a variable duty cycle provides a flexible means of extracting data necessary for capturing complete sets of solar panel characteristics.

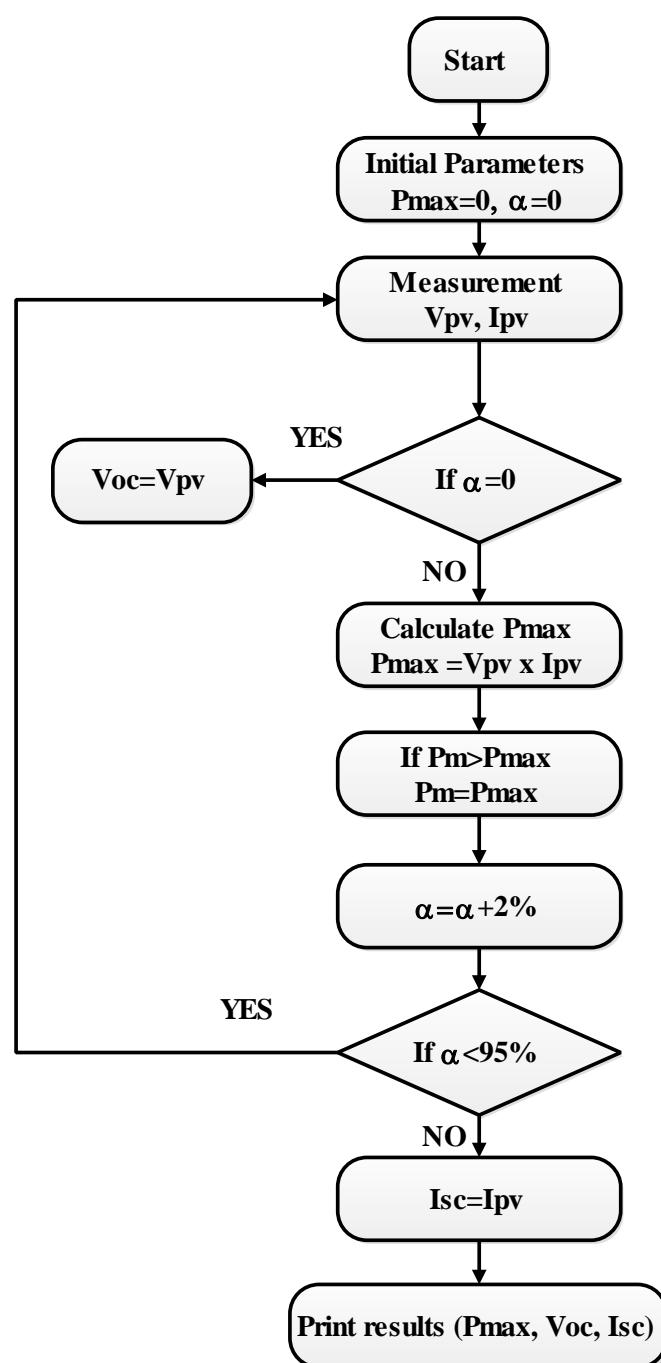


Figure 6. Algorithm for extracting real parameters

3.2. Temperature and Radiation Impact on PV Panels

Figure 7 shows the relationship between time and open-circuit voltage (V_{pv}) for different temperature values under constant irradiation of 1000 W/m^2 . As the temperature increases, the V_{pv} curves shift downward. This indicates that the maximum output voltage of the PV panel decreases at higher temperatures. This phenomenon is mainly due to increased carrier recombination and reduced carrier mobility in the semiconductor material at high temperatures.

Figure 8 shows the output power (P) of the PV panel over time for different temperature values. It is obvious that as the temperature increases, the maximum output power decreases. This is mainly attributed to two factors: (1) the decrease in V_{oc} , as observed in **Figure 7**, and (2) the increase in internal losses within the panel, such as resistive losses and junction leakage current, which become more significant at higher temperatures.

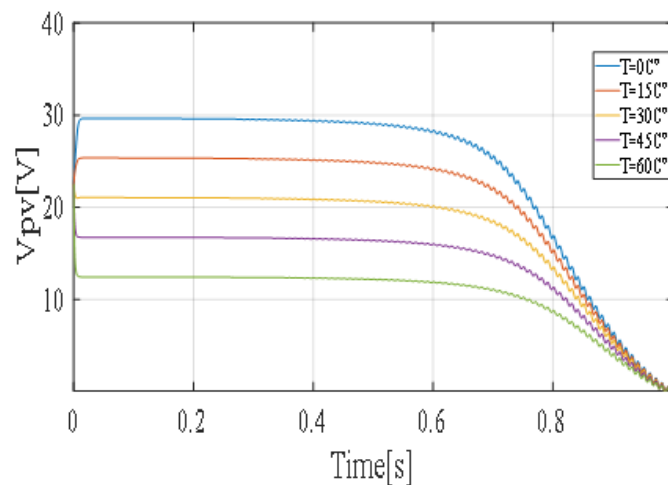


Figure 7. Characteristics (V_{pv}) for different temperature values at $G=1000\text{W/m}^2$.

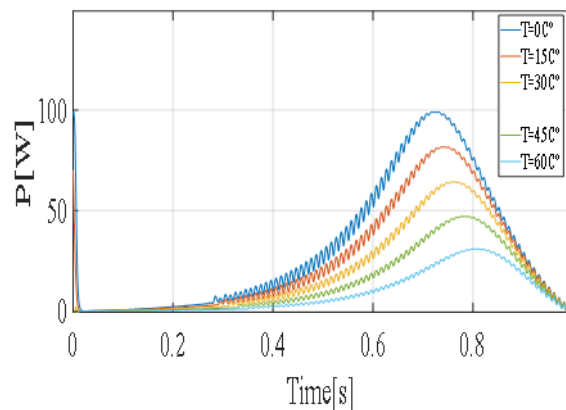


Figure 8. Characteristics (P) for different temperature values at $G=1000\text{W/m}^2$

Figure 9 shows the short-circuit current (I_{pv}) as a function of time for different temperature values. Although there is a slight increase in I_{pv} with increasing temperatures, it is generally less pronounced compared to the decrease in V_{oc} . This increase can be attributed to the reduced resistance of the semiconductor material at higher temperatures, which leads to a slightly higher current flow.

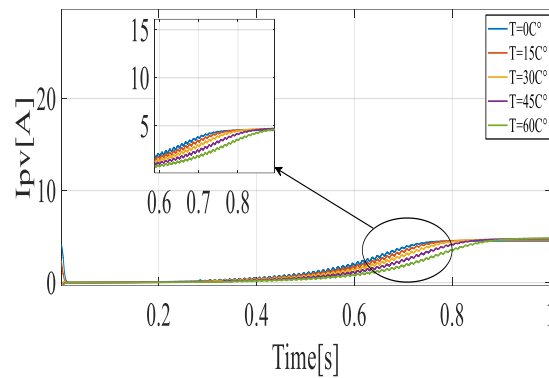


Figure 9. Characteristics (I_{pv}) for different temperature values at $G=1000W/m^2$

Figure 10 shows the power-voltage (P-V) curves of the PV panel for different temperatures. As the temperature increases, the MPP shifts to lower voltages and currents. This is a combined effect of the decrease in V_{oc} and the increase in I_{pv} . The maximum power point represents the optimum operating condition of the PV panel, and its shift to lower voltages and currents indicates that the efficiency of the panel is reduced at higher temperatures.

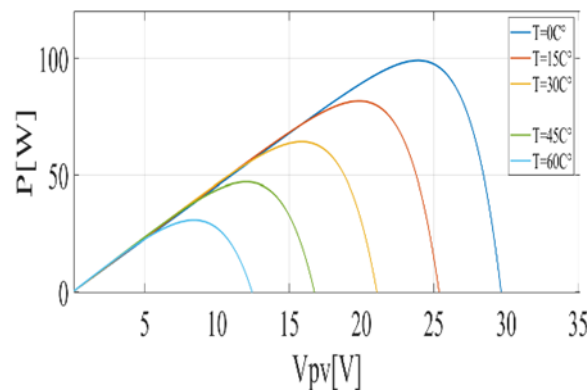


Figure 10. Characteristics (P-V) for different temperature values at $G= 1000w/m^2$

Figure 11 illustrates the relationship between time and V_{pv} for different irradiation levels at a constant temperature of 25 °C. As the irradiation increases, the V_{pv} curves shift upwards. This is due to the increased generation of electron-hole pairs in the PV panel as more photons are absorbed. A higher number of charge carriers results in a higher open circuit voltage.

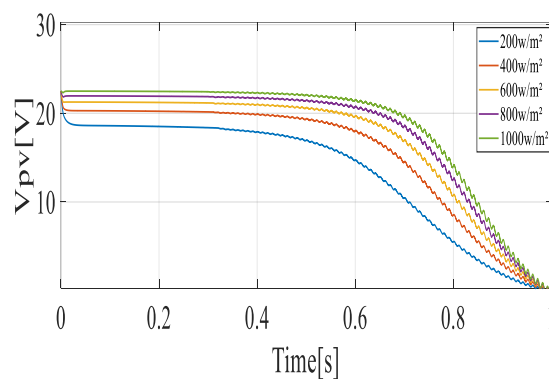


Figure 11. Characteristics (V_{pv}) for different radiation values at a temperature of 25°C

Figure 12 shows the output power (P) of the PV panel for different irradiation levels at a constant temperature. As the irradiation increases, the peak output power also increases significantly. This is a direct consequence of the increased number of photons available for energy conversion.

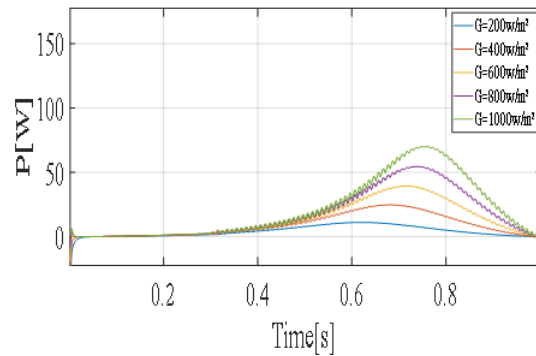


Figure 12. Characteristics (P) for different radiation values at a temperature of 25°C

Figure 13 shows the short-circuit current (I_{pv}) as a function of time for different irradiation levels. Just like V_{pv} , I_{pv} increases with increasing irradiation. This is due to the increased generation of charge carriers, which leads to a higher current flow.

Figure 14 shows the P-V curves of the PV panel for different irradiation levels. As the irradiation increases, the MPP shifts to higher voltages and currents. This is a combined effect of the increase in V_{oc} and I_{pv} . The higher MPP indicates that the efficiency of the PV panel improves with higher irradiation levels.

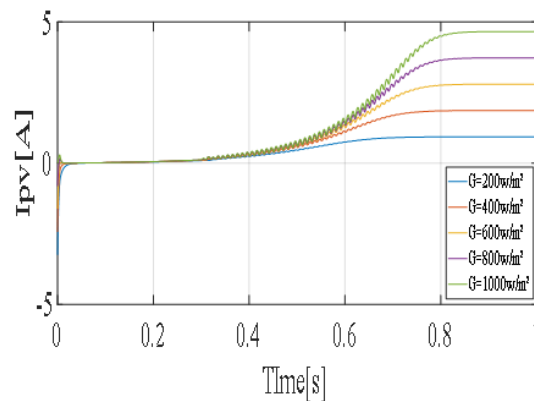


Figure 13. Characteristics (I_{pv}) for different radiation values at a temperature of 25°C

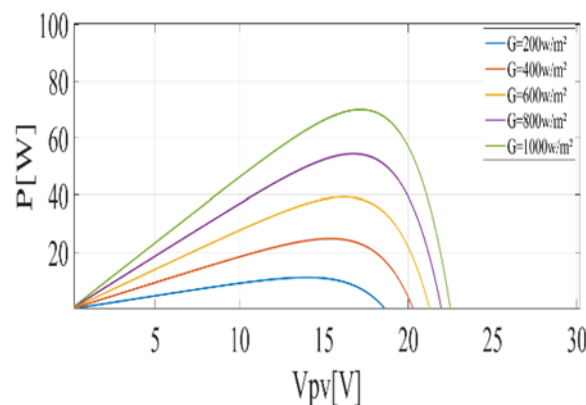


Figure 14. Characteristics (P-V) for different radiation values at a temperature of 25°C

3.3. Experimental Validation

This part presents an experimental validation of the proposed strategy that aims at assessing conformity and quality between two different states of PV systems. The validity of this strategy is verified using a detailed experimental setup. The experimental test bench comprises a DC/DC back boost converter connected to a PV panel and resistive load (R load). A key component in this system is the converter, which is constructed using FGH40N60 MOSFETs, inductance, capacitance, and diode. For the implementation of control logic, a Texas Instruments TMS320F28379D digital signal processor (DSP) is used whereby the control system operates at a 50 kHz switching frequency. The IGBT switching devices are given signals from three digital outputs originating from DSP while in the case of MOSFETs, only one signal is required since the gate driver based on an isolated transformer needs only one signal for control. By using this gate driver, one can create control signals for either high-side or low-side PV systems. Also, voltage sensors as well as current sensors are included to monitor output PV current and voltage respectively.

These tests were done to make sure that the proposed strategy is valid. They measured the quality and conformity of two different types of panels; one that was made according to industry standards, and another that had been intentionally created with defects and non-standard features. In addition, both panels were exposed to different levels of solar power input as well as temperature variations. This information is presented in **Table 3**.

Table 3. Comparative Analysis of PV Panel Performance: Healthy vs. Faulty States

Condition		Healthy PV			Faulty PV		
Solar power [w]	Temperature [°]	V_{oc} [V]	I_{sc} [A]	P_{max} [w]	V_{oc} [V]	I_{sc} [A]	P_{max} [w]
845	35	20.97	4.18	72.20	20.63	2.11	29.12
915	38	21.32	4.32	75.30	20.92	2.27	33.15
922	40	21.22	4.29	74.80	20.82	2.24	32.45
890	43	21.10	4.25	73.55	20.75	2.18	30.24
885	46	20.92	4.15	71.50	20.52	2.05	28.15
902	48	20.95	4.17	71.94	20.58	2.08	28.78
878	50	20.76	4.12	70.44	20.45	2.01	27.58

This study aimed at validating the proposed strategy through experimental trials on PV modules under normal and faulty states using V_{oc} (open-circuit voltage) of 22.5V, I_{sc} (short circuit current) of 4.66A, P_{max} (maximum power) of 80W as manufacturing parameters with thermal inputs varied by solar power ranging from 845-902W at temperatures between 35°C-48°C for state 1 representing healthy PV panels where performance declined significantly dropping down between electrical power outputs of 70.44W-75.30W while state 2 simulating faultiness observed more substantial fall off showing electric output powers within range: 28.15W–33.15W. Moreover, corresponding V_{oc} , I_{sc} , and P_{max} values further confirmed this efficiency reduction effect due to faults on the PV module which led to the decreased voltage drop across its terminals alongside a decline in current produced by them respectively. These findings highlight how effective this strategy could be when it comes to the detection or explanation of various types of solar panels used in different systems for energy generation.

4. CONCLUSION

This study critically addresses the quality assessment of PV panels by analyzing their efficiency and electrical power under varying environmental conditions. A sophisticated

algorithm was developed to extract and analyze PV panel voltage and current data in a complex manner, allowing the identification of key parameters such as open circuit voltage (V_{oc}), short circuit current (I_{sc}), and peak electrical power. These parameters were compared with the input power to accurately determine the panel efficiency. The novelty of this approach lies in its real-time implementation using a DC/DC (buck-boost) converter equipped with precise voltage and current sensors and running on a TMS320f379D board, linking theoretical knowledge with practical results. Experimental results demonstrate that temperature and irradiation significantly influence PV performance: a 10°C increase in temperature results in a 5–10% decrease in output power, while a 100 W/m² increase in irradiation results in a 10–15% increase in output power. The study highlights the importance of considering both temperature and irradiation variations to optimize PV system design and operation, providing a robust method to assess PV panel quality in real time.

5. AUTHORS' NOTE

The authors declare that there is no conflict of interest regarding the publication of this article. Authors confirmed that the paper was free of plagiarism.

6. REFERENCES

- Atiyah, H., Boukattaya, M., and Bensalem, F. (2023). Principal component analysis-based shading defect identification and categorization in standalone PV systems using I-V curves. *International Journal of Energetica*, 8(2), 44-53.
- Bharadwaj, P., Chaudhury, K., and John, V. (2016). Sequential optimization for PV panel parameter estimation. *IEEE Journal of Photovoltaics*, 6, 1261-1268.
- Dhimish, M., Holmes, V., Mehrdadi, B., and Dales, M. (2018). Comparing Mamdani Sugeno fuzzy logic and RBF ANN network for PV fault detection. *Renewable Energy*, 117, 257-274.
- Eskandari, A., Milimonfared, J., and Aghaei, M. (2021). Fault detection and classification for photovoltaic systems based on hierarchical classification and machine learning technique. *IEEE Transactions on Industrial Electronics*, 68, 12750-12759.
- Fadhel, S., Delpha, C., Diallo, D., Bahri, I., Migan, A., Trabelsi, M., and Mimouni, M. F. (2019). PV shading fault detection and classification based on I–V curve using principal component analysis: Application to isolated PV system. *Solar Energy*, 179, 1-10.
- Ghodbane, M., Bessous, N., Boumeddane, B., and Lahrech, K. (2023). Optimal tilt angle for photovoltaic panels in the Algerian region of El-Oued in the spring season: An experimental study. *International Journal of Energetica*, 8(1), 24-30.
- Hong, Y.-Y., and Pula, R. A. (2022). Methods of photovoltaic fault detection and classification: A review. *Energy Reports*, 8, 5898-5929.
- Ji, D., Zhang, C., Lv, M., Ma, Y., and Guan, N. (2017). Photovoltaic array fault detection by automatic reconfiguration. *Energies*, 10(699), 1-13.
- Kattakayam, T., Khan, S., and Srinivasan, K. (1996). Diurnal and environmental characterization of solar photovoltaic panels using a PC-AT add-on plug-in card. *Solar Energy Materials and Solar Cells*, 44, 25-36.

- Kim, G., Lee, W., Bhang, B., Choi, J., and Ahn, H. (2021). Fault detection for photovoltaic systems using multivariate analysis with electrical and environmental variables. *IEEE Journal of Photovoltaics*, *11*, 202-212.
- Largot, S., Bessous, N., Ghodbane, M., Boumeddane, B., Lahrech, K., and Aswad, R. (2024). Dust accumulation effects on the performance of photovoltaic panels: An experimental study in the Algerian region of El-Oued. *International Journal of Energetica*, *9*(1), 01-09.
- Manno, D., Cipriani, G., Ciulla, G., Di Dio, V., Guarino, S., and Lo Brano, V. (2021). Deep learning strategies for automatic fault diagnosis in photovoltaic systems by thermographic images. *Energy Conversion and Management*, *241*, 114315.
- Medekhel, L., Srairi, K., and Labiod, C. (2022). Experimental study of temperature effects on the photovoltaic solar panels performances in Algerian desert. *International Journal of Energetica*, *7*(1), 18-22.
- Momeni, H., Sadoogi, N., Farrokhifar, M., and Gharibeh, H. (2020). Fault diagnosis in photovoltaic arrays using GBSSL method and proposing a fault correction system. *IEEE Transactions on Industrial Informatics*, *16*, 5300-5308.
- Movla, H., Shahalizad, A., and Abad, A. (2015). Influence of active region thickness on the performance of bulk heterojunction solar cells: Electrical modeling and simulation. *Optical and Quantum Electronics*, *47*, 621-632.
- Paul, M., Mahalakshmi, R., Karuppasamyandian, M., Bhuvanesh, A., and Ganesh, R. (2016). Fault identification and islanding in DC grid connected PV system. *Circuits and Systems*, *7*, 2904-2915.
- Roger, J., and Maguin, C. (1982). Photovoltaic solar panels simulation including dynamical thermal effects. *Solar Energy*, *29*, 245-256.
- Tina, G. M., Cosentino, F., and Ventura, C. (2015). Monitoring and diagnostics of photovoltaic power plants. *Renewable Energy Services Manual*, *2*, 505-516.
- Trypanagnostopoulos, G., Kavga, A., Souliotis, M., and Tripanagnostopoulos, Y. (2017). Greenhouse performance results for roof installed photovoltaics. *Renewable Energy*, *111*, 724-731.
- Vinod, P. (2008). Power loss calculation as a reliable methodology to assess the ohmic losses of the planar ohmic contacts formed on the photovoltaic devices. *Journal of Materials Science: Materials in Electronics*, *19*, 594-601.
- Vinod, R. K., and Singh, S. K. (2018). Solar photovoltaic modeling and simulation: As a renewable energy solution. *Energy Reports*, *4*, 701-712.
- Yang, Y., Blaabjerg, F., and Zou, Z. (2013). Benchmarking of grid fault modes in single-phase grid-connected photovoltaic systems. *IEEE Transactions on Industry Applications*, *49*, 2167-2176.
- Zagrouba, M., Sellami, A., Bouaïcha, M., and Ksouri, M. (2010). Identification of PV solar cells and modules parameters using the genetic algorithms: Application to maximum power extraction. *Solar Energy*, *84*, 860-866.

- Zaimi, M., Achouby, H., Ibral, A., and Assaid, E. (2019). Determining combined effects of solar radiation and panel junction temperature on all model-parameters to forecast peak power and photovoltaic yield of solar panel under non-standard conditions. *Solar Energy*. 191, 341-359.
- Zhang, Z., Ma, M., Wang, H., Wang, H., Ma, W., and Zhang, X. (2021). A fault diagnosis method for photovoltaic module current mismatch based on numerical analysis and statistics. *Solar Energy*, 225, 221-236.
- Zhao, Y., Palma, J., Mosesian, J., Lyons, R., and Lehman, B. (2013). Line-line fault analysis and protection challenges in solar photovoltaic arrays. *IEEE Transactions on Industrial Electronics*, 60, 3784-3795.
- Zhu, H., Wang, H., Kang, D., Zhang, L., Lu, L., Yao, J., and Hu, Y. (2019). Study of joint temporal-spatial distribution of array output for large-scale photovoltaic plant and its fault diagnosis application. *Solar Energy*. 181, 137-147.